

> REPLACE THIS LINE WITH YOUR MANUSCRIPT ID NUMBER (DOUBLE-CLICK HERE TO EDIT) <

# All-Polarization-Maintained Microwave Photonic Phase Detector Based on Dual-Polarization Dual-Drive Mach-Zehnder Modulator

Kunlin Shao, Shuo Liu, Penghui Gao, Yamei Zhang\*, *Member, IEEE*, Zhongyang Xu, *Member, IEEE*, Hui Wang, and Shilong Pan, *Fellow, IEEE*

**Abstract**—An all-polarization-maintained microwave photonic phase detector (MPPD) based on a dual-polarization dual-drive Mach-Zehnder modulator (DP-DMZM) is demonstrated to detect the phase difference between a microwave signal and an optical pulse train. The robustness of the MPPD can be significantly improved with the all-polarization-maintained structure. A proof-of-concept experiment is carried out. An 8.032-GHz dielectric resonator oscillator (DRO) is locked to an optical pulse train through this MPPD with its phase noise reducing from -109.68 dBc/Hz to -135.41 dBc/Hz at 10-kHz offset frequency. The DP-DMZM-based MPPD shows that the minimum value of the noise floor is around -154 dBc/Hz, and the integrated residual timing jitters from 100 Hz to 100 kHz, 1 MHz, and 3 MHz are 276 as, 696 as, and 2.50 fs, respectively. The MPPD has good stability against external vibrations and stresses.

**Index Terms**—Microwave photonics phase detector, femtosecond pulse, MLL.

## I. INTRODUCTION

Phase detectors play an important role in applications such as radar [1], sampling systems [2], timing synchronization and distribution systems [3], etc. A phase detector is traditionally used to extract the phase difference between a microwave signal and an electronic reference clock. However, due to the large timing jitter and broad pulse width of the electronic clock, the phase detection accuracy of the phase detector is generally poor, which would worsen the synchronization or phase-locking performance of the following processing. Owing to the ultra-low timing jitter and abundant frequency components of a femtosecond optical pulse provided by a mode-locked laser (MLL) [4]-[5], a femtosecond optical pulse is considered as a promising reference clock for timing synchronization and phase-locking applications. Therefore, a microwave photonic phase detector (MPPD) is highly desired to extract the phase difference between a microwave signal and an optical pulse. Compared with the traditionally electronic phase detector, the MPPD shows a high phase detection accuracy and can be

employed to achieve a local oscillation signal with an ultra-low phase noise [6]-[7]. Thus, the MPPD has attracted much attention during the past decade, and extensive efforts have been devoted to realizing the MPPD [8]. According to the structure, MPPDs can be categorized into two types. One is Sagnac-loop structure, and the other is straight-forward structure.

For the Sagnac-loop structure MPPD, the key is to build a Sagnac loop embedded with a nonreciprocal device, in which two counter-propagated signals exist and a phase difference is introduced to them via the nonreciprocal device. Therefore, phase interference would occur at the Sagnac loop's output, and the phase error between the optical pulse and the microwave signal can be extracted.

The first Sagnac-loop-based MPPD was realized using a spatial structure [9], in which a quarter-wave plate is employed to introduce the phase difference between the two counter-propagated signals, and a 2-GHz signal is synchronized to an MLL. Since the spatial structure is bulky and sensitive to environmental variations, it has a relatively high residual noise. To deal with this problem, fiber-based MPPDs were then put forward [10]-[13]. A nonreciprocal phase shifter or a 3×3 optical coupler was employed, and a residual noise of <-150 dBc/Hz was obtained.

For the straight-forward structure MPPD, two systems were reported. In [14], a polarization modulator (PoIM) based MPPD was reported. By carefully adjusting the polarization controller (PC) in the structure, a relatively low noise floor of -150 dBc/Hz can be obtained. However, the existence of the PC makes the system sensitive to variations of the external stress, vibrations and temperature, which may degrade the long-term stability. In [15], a dual-output Mach-Zehnder modulator (DOMZM) based MPPD was proposed. By biasing the DOMZM at the quadrature transmission point, the power difference between the two outputs is proportional to the phase difference between the microwave signal and the optical pulse. As a result, the phase difference can be extracted. A 10-GHz signal is

Manuscript received xx xx, xxxx; revised xx xx, xxxx and xx xx, xxxx; accepted xx xx, xxxx. Date of publication xx xx, xxxx; date of current version xx xx, xxxx. This work was supported in part by the National Natural Science Foundation of China under Grant (61901215, 62171219), and in part by the Jiangsu Natural Science Foundation under Grant BK20190404. (Corresponding author: Yamei Zhang).

Kunlin Shao, Shuo Liu, Penghui Gao, Yamei Zhang, Zhongyang Xu, and

Shilong Pan are with the Key Laboratory of Radar Imaging and Microwave Photonics (Nanjing Univ. Aeronaut. Astronaut.), Ministry of Education, Nanjing University of Aeronautics and Astronautics, Nanjing 210016, China, and Hui Wang is with Shanghai Institute of Satellite Engineering, Shanghai, China, (e-mail: zhang\_ym@nuaa.edu.cn).

Color versions of one or more of the figures in this article are available online at <http://ieeexplore.ieee.org>  
Digital Object Identifier xxxxxx.

synchronized to an MLL, and the noise floor of this system is only about -150 dBc/Hz.

In this Letter, a dual-polarization dual-drive Mach-Zehnder modulator (DP-DMZM) based MPPD is put forward and experimentally demonstrated. Compared to that in [16] we proposed before, an all-polarization-maintaining structure is employed and the performance is significantly improved. This MPPD shows a locking bandwidth of more than 1 MHz, and the residual noise floor reaches -154 dBc/Hz. An 8.032-GHz dielectric resonator oscillator (DRO) is locked to an MLL, and at 10-kHz offset frequency, the phase noise reduces from -109.68 dBc/Hz to -135.41 dBc/Hz. From 100 Hz to 1 MHz, the integrated residual timing jitter is about 696 as.

## II. PRINCIPLE

Fig. 1(a) gives the setup of the proposed MPPD, consisting a DP-DMZM, a polarization maintaining polarization beam splitter (PM-PBS), and a balanced photodetector (BPD). The MLL generates an optical pulse train, which is sent to the DP-DMZM as an optical timing reference. The waveform bandwidth of the MLL can cover tens of nanometers, so the transform-limited pulse width is less than 100 fs. This characteristic lets the pulse train be denoted as,

$$E_{\text{MLL}}(t) = \sqrt{P_{\text{peak}}} \sum_{n=0}^{\infty} \delta\left(t - \frac{n}{f_{\text{rep}}}\right) \quad (1)$$

where  $P_{\text{peak}}$  is the peak power of a single pulse, and  $f_{\text{rep}}$  is the repetition rate of the optical pulse. The microwave signal emitted from the DRO can be written as

$$s(t) = a \sin(2\pi N f_{\text{rep}} t + \varphi) \quad (2)$$

where  $a$  is the amplitude of the output of the DRO,  $\varphi$  is the phase of the DRO that relative to the optical pulse of the MLL, and  $N f_{\text{rep}}$  is the frequency of the DRO which indicates that the

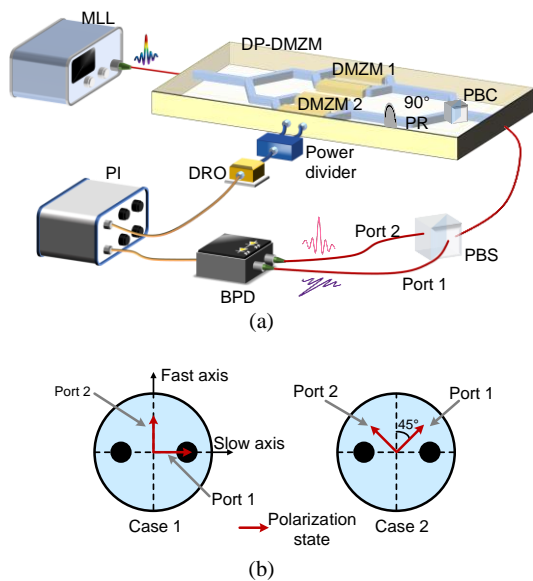


Fig. 1. (a) Schematic diagram of the proposed MPPD. MLL: mode-locked laser; DP-DMZM: dual-polarization dual-drive Mach-Zehnder modulator; PR: polarization rotator; PBC: polarization beam combiner; PBS: polarization beam splitter; DRO: dielectric resonator oscillator; BPD: balanced photodetector; PI: proportional-integral controller. (b) Polarization states in port 1 and port 2 of the PM-PBS.

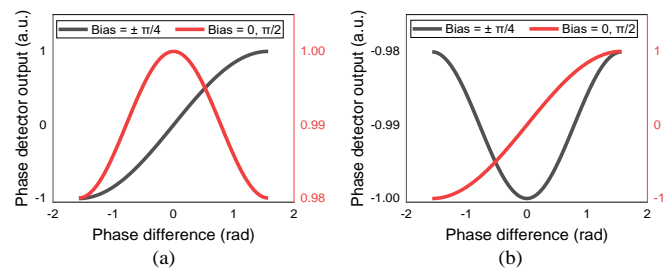


Fig. 2. The detection curves under different bias points and polarization splitting angles. Black lines: result under quadrature bias point. Red lines: result under maximum and minimum bias point. (a) Polarization splitting angle is  $0^\circ$ . (b) Polarization splitting angle is  $45^\circ$ .

microwave frequency should equal one harmonic frequency of the MLL.

The microwave signal is then split into two paths to drive the two sub-DMZMs of the DP-DMZM. The outputs of the two sub-DMZMs are combined by a polarization beam combiner (PBC) after the state of polarization (SOP) of the signal from sub-DMZM2 being rotated by  $90^\circ$ . The output of the DP-DMZM can be expressed as,

$$\begin{bmatrix} E_x \\ E_y \end{bmatrix} \propto \sqrt{P_{\text{peak}}} \begin{bmatrix} \cos\left(\frac{\sqrt{2}\pi a}{2V_\pi} \sin\varphi + \theta_x\right) \\ \cos\left(\frac{\sqrt{2}\pi a}{2V_\pi} \sin\varphi + \theta_y\right) \end{bmatrix} \sum_{n=0}^{\infty} \delta\left(t - \frac{n}{f_{\text{rep}}}\right) \quad (3)$$

where  $E_x$  and  $E_y$  denote the signals along the slow axis and fast axis, respectively,  $\theta_x$  and  $\theta_y$  are the phase biases introduced by the DC voltage applied to each sub-DMZMs, and  $V_\pi$  is the half-wave voltage of the DP-DMZM. The output fiber of the DP-DMZM is a polarization maintaining fiber (PMF).

A PM-PBS is used to split the optical pulse trains along the two orthogonal polarization directions into two paths. The two outputs of the PBS can be aligned to the principal axes of the DP-DMZM as Case 1 shown in Fig. 1(b), or be aligned to have an angle of  $45^\circ$  to the principal axes of the DP-DMZM as Case 2 shown in Fig. 1(b). To simplify the analysis, only Case 2 is taken into consideration, so the outputs of the PBS can be written as,

$$\begin{bmatrix} E_1 \\ E_2 \end{bmatrix} \propto \begin{bmatrix} E_x + E_y \\ E_x - E_y \end{bmatrix} \quad (4)$$

By adjusting the DC biases of the DP-DMZM, the phase biases of the sub-DMZMs can be controlled to be  $\pi/2$  and  $0$ , respectively. Then, the average optical power difference between the two ports of the PBS can be written as,

$$\Delta P \propto \sin\left(\frac{\sqrt{2}\pi a}{V_\pi} \sin\varphi\right) \approx \frac{\sqrt{2}\pi a}{V_\pi} \varphi \quad (5)$$

From Eq. (5), it is seen that the power difference is proportional to the phase difference  $\varphi$ , and Fig. 2 gives the normalized phase detection curves under the two cases, indicating that both cases can detect the phase difference correctly at appropriate bias points. With the phase difference, the DRO can be locked to the optical pulse by a proportional-integral (PI) controller.

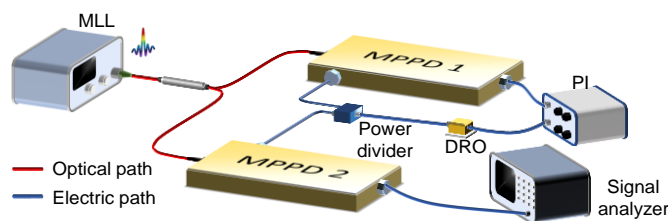


Fig. 3. The experimental setup for residual noise measurement.

### III. EXPERIMENTAL RESULTS

Based on the scheme in Fig. 1(a), an experiment is carried out to study the performance of the MPPD, and another same MPPD is established to measure the residual noise, namely the noise floor. The whole setup is depicted in Fig. 3.

A reference optical pulse train with 100.4-MHz repetition rate is generated by an MLL (Menlo, C-Fiber). The pulse width is less than 100 fs, and its power is about 20 dBm. A 50:50 PM optical coupler then splits the pulse train into two paths. Each pulse train is applied to a DP-DMZM (Fujitsu, FTM 7980), of which both the input and output fibers are PMFs. An 8.032-GHz microwave generated by a DRO (Hittite, HMC-C200 8000) is applied to the two DP-DMZMs after being split by an RF power divider. The microwave power to each MPPD is about 6 dBm. The bias points of each sub-DMZM are set to  $\pi/2$  and 0 by adjusting the DC voltage. The PM-PBS used here is as the one in Case 2 in Fig. 1(b). The optical power injected into the BPD (Thorlabs, PDB450C) is about 1 dBm. The output of MPPD1 is fed back to the DRO through a PI (New Focus, LB 1005) to lock the microwave signal to the MLL, and the output of MPPD2 is captured by a signal analyzer to obtain the residual noise between the locked microwave and the optical pulse.

The phase noise characteristics of the system are firstly investigated with results depicted in Fig. 4(a), in which the phase noise curves are obtained by a phase noise analyzer (Rohde & Schwarz, FSWP). Curve (i) and curve (ii) in Fig. 4(a) are the phase noises of the free running DRO and the locked DRO that measured without any optimization, respectively. As can be seen, for the synchronized DRO, the phase noise decreases by more than 25 dB at 10-kHz offset frequency, i.e., from -109.68 dBc/Hz to -135.21 dBc/Hz, and the phase noise reaches -146.66 dBc/Hz at a frequency offset of 100 kHz, indicating that, the phase noise performance of the DRO has been significantly improved after phase locking to an MLL.

To further improve the phase noise performance, the power of the microwave signal is amplified to 21 dBm before driving the DP-DMZM, and curve (iii) shows its phase noise. As can be seen, the phase noise at 10-kHz offset frequency is -135.41 dBc/Hz, showing negligible change, while that the phase noise becomes lower at higher offset frequencies. For example, at 100-kHz offset frequency, the phase noise reaches -152.02 dBc/Hz, around 6 dB improvement achieved. The locking bandwidth is about 2 MHz with a resonant peak around it. The intersection of curve (i) and curve (iii) around 300 kHz determines the best locking bandwidth.

To confirm the excellent phase noise performance of the

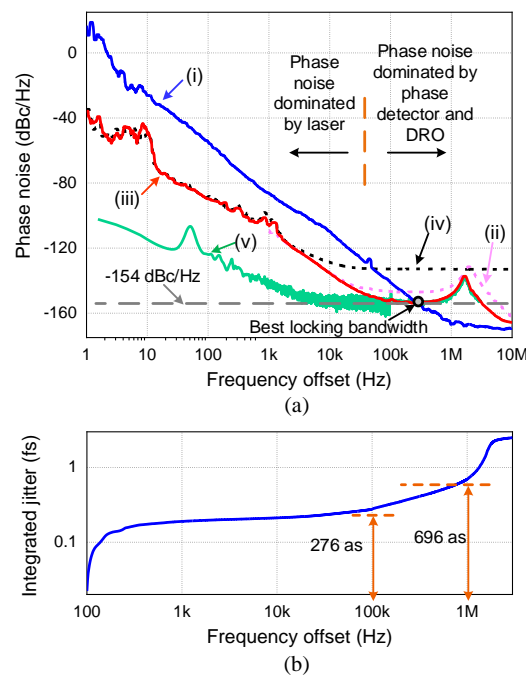


Fig. 4. (a) Noise spectra. Curve (i), phase noise of the free running microwave; Curve(ii), phase noise of the locked microwave without amplification; Curve(iii), phase noise of the locked microwave with amplification; Curve(iv), phase noise of MLL by beat in a common PD; Curve (v), residual noise between the locked microwave and the optical pulse. (b) Integrated residual timing jitter between the locked microwave and the optical pulse.

MPPD, the phase noise of the 80<sup>th</sup> harmonic of the optical pulse repetition rate is also observed by directly beating the pulse train in a common PD (Finisar, XPDV2120), as shown as curve (iv) of Fig. 4(a). The optical injection power is about -2.6 dBm to assure that the optical peak power will not destroy the PD, and the output power of the PD is amplified to be about -15 dBm. From curve (iv) we can see that, the locked DRO follows the phase noise of the 80<sup>th</sup> harmonic at low offset frequencies, but at the higher offset frequencies, it is limited to be only -133 dBc/Hz, which is mainly due to the excess noise introduced by PD at the optical-to-electrical conversion process and the poor SNR induced by the low conversion efficiency. Therefore, we can conclude that, using an MPPD to get a low phase noise microwave signal shows better performance.

Then the residual noise between the locked microwave and the optical pulse is measured to evaluate the detection resolution of the MPPD, as shown as curve (v) in Fig. 4(a). The part under 100-kHz offset is measured by a 200-kHz data acquisition card, and the part above 100 kHz is measured by a spectrum analyzer. Curve (iv) and curve (v) intersect at around 40 kHz. Below 40-kHz offset, the phase noise of the locked microwave is dominated by the optical pulse, while above 40-kHz offset, it is limited by the noise floor of the MPPD. The minimum value of the noise floor is around -154 dBc/Hz, which improves by 4 dB more than that of the DOMZM- (PoIM-) based MPPD in [14] and [15], and 21 dB more than that of the direct photodetection condition. Since the DC component cannot be eliminated completely, the residual noise under 100 Hz may be not accurate. Therefore, the residual timing jitter is

integrated from 100 Hz to 3 MHz, and the curve is shown in Fig. 4(b). It is seen that the integrated jitters from 100 Hz to 100 kHz, 1 MHz and 3 MHz are about 276 as, 696 as and 2.50 fs, respectively. The sharp increasing of the jitter after 1 MHz is caused mainly by the resonant peak of the MPPD. This can be reduced by using a lead compensator [15] in the feedback loop.

To verify the robustness of the MPPD, disturbance is exerted to the PM-PBS to observe the variations of the spectrum of the DRO. Fig. 5(a) is the spectrum of the DRO without any disturbance, and Fig. 5(b) and (c) are the spectra of the DRO when the PM-PBS is shaking and fiber-bending, respectively. As can be seen from Fig. 5(a) to (c), the locking bandwidth reduces dramatically, but it is still under locking status, and the signal remains about 110 dB higher than the noise floor with a 100-Hz resolution bandwidth (RBW). When the perturbation is lifted, the spectrum will recover back to that in Fig. 5(a). We also observed that, when the fiber is bent too much, the MPPD will loss locking, but it can be locked again after the perturbation disappears. It is also found in the experiment that reducing the gain of the PI can make the locking more robust against the perturbation at the cost of the locking range. For comparison, the PM-PBS is replaced by a single-mode fiber PBS (SMF-PBS), and a PC is inserted between it and the DP-DMZM. Fig. 5(d) shows the signal spectrum of the DRO. As can be seen, the signal is also about 110 dB higher than the noise floor with a 100-Hz RBW, and the locking range reaches 2.5 MHz by adjusting the PC carefully. However, when the SMF-PBS is shaking, the DRO would be unlocked as shown as Fig. 5(e), and it cannot recover after the disturbance lifted. This comparison proves that the polarization maintaining structure makes the system more robust, giving the possibility for practical applications.

#### IV. CONCLUSION

In conclusion, an MPPD based on a DP-DMZM using all polarization maintaining devices is proposed and demonstrated. The minimum noise floor of this MPPD is around -154 dBc/Hz. A DRO is locked to an MLL through this MPPD, and the phase noise improves from -109.68 dBc/Hz to -135.41 dBc/Hz at 10-kHz offset frequency. The integrated residual timing jitter is about 696 as from 100 Hz to 1 MHz. The proposed all polarization-maintained MPPD shows outstanding robustness against the external vibrations and stresses.

#### REFERENCES

- [1] P. Ghelfi, F. Laghezza, F. Scotti et al., "A fully photonics-based coherent radar system," *Nature*, vol. 507, no. 7492, pp. 341–345, Mar. 2014.
- [2] A. Oz and K. Peker, "Synchronizing sample clocks of a data converter array," *Analog Devices, Inc., Tech. Rep.*
- [3] H. Zhang, L. He, X. Li, Y. Xiao, P. Qu, and L. Sun, "Wideband microwave frequency distribution for multi-access along a single fiber link," *J. Lightw. Technol.*, vol. 38, no. 7, pp. 1688–1692, Apr. 2020.
- [4] Y. Song, C. Kim, K. Jung, H. Kim, and J. Kim, "Timing jitter optimization of mode-locked Yb-fiber lasers toward the attosecond regime," *Opt. Express*, vol. 19, no. 15, pp. 14518–14525, Jul. 2011.
- [5] N. Kuse, J. Jiang, C.-C. Lee, T. R. Schibli, and M. E. Fermann, "All polarization-maintaining Er fiber-based optical frequency combs with nonlinear amplifying loop mirror," *Opt. Express*, vol. 24, no. 3, pp. 3095–3102, Feb. 2016.

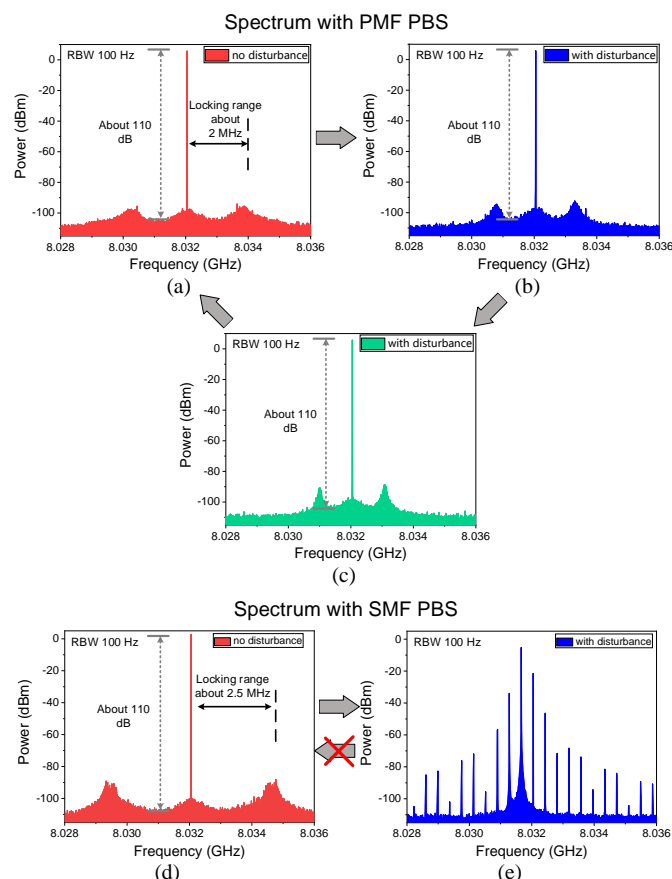


Fig. 5. Spectrum of the microwave generated by the DRO. (a)-(c) Spectra of the microwave when a PM-PBS is used. (d)-(e) Spectra of the microwave when a SMF-PBS is used.

- [6] S. L. Pan and Y. M. Zhang, "Microwave Photonic Radars", *J. Lightw. Technol.*, vol. 38, no. 19, pp. 5450-5484, Oct. 2020.
- [7] J. Wei, D. Kwon, S. Zhang, S. Pan, and J. Kim, "All-fiber-photonics-based ultralow-noise agile frequency synthesizer for X-band radars," *Photon. Res.*, vol. 6, no. 1, pp. 12–17, Jan. 2018.
- [8] M. Lessing, H. S. Margolis, C. T. Brown, P. Gill, and G. Marra, "Suppression of amplitude-to-phase noise conversion in balanced optical-microwave phase detectors," *Opt. Express*, vol. 21, no. 22, pp. 27057–27062, Nov. 2013.
- [9] J. Kim, F. X. Kartner, and M. H. Perrott, "Femtosecond synchronization of radio frequency signals with optical pulse trains," *Opt. Lett.*, vol. 29, no. 17, pp. 2076–2078, Sep. 2004.
- [10] J. Kim, F. X. Kartner, and F. Ludwig, "Balanced optical-microwave phase detectors for optoelectronic phase-locked loops," *Opt. Lett.*, vol. 31, pp. 3659–3661, Dec. 2006.
- [11] K. Jung and J. Kim, "Subfemtosecond synchronization of microwave oscillators with mode-locked Er-fiber lasers," *Opt. Lett.*, vol. 37, no. 14, pp. 2958–2960, Jul. 2012.
- [12] K. Jung, J. Shin, and J. Kim, "Ultralow phase noise microwave generation from mode-locked Er-Fiber lasers with subfemtosecond integrated timing jitter," *IEEE Photon. J.*, vol. 5, no. 3, Paper 5500906, Jun. 2013.
- [13] C. Jeon, Y. Na, B. Lee, and J. Kim, "Simple-structured, subfemtosecond-resolution optical-microwave phase detector," *Opt. Lett.*, vol. 43, no. 16, pp. 3997–4000, Aug. 2018.
- [14] J. Wei, S. Zhang, J. Kim, and S. Pan, "Compact phase detector for optical-microwave synchronization using polarization modulation," *J. Lightw. Technol.*, vol. 36, no. 19, pp. 4267–4272, Oct. 2018.
- [15] M. Bahmanian, J. C. Scheytt, "A 2–20-GHz ultralow phase noise signal source using a microwave oscillator locked to a mode-locked laser," *IEEE Trans. Microw. Theory Techn.*, vol. 69, no. 3, pp. 1635-1645, Mar. 2021.
- [16] K. Shao, S. Liu, P. Gao, et al. "A microwave photonic phase detector based on a dual-polarization dual-drive Mach-Zehnder modulator," in *Proc. 26th OptoElec. and Commun. Conf. (OECC)*, Hong Kong, China, 2021, M3E. 3.